Nonlocal buckling behavior of bonded double-nanoplate-systems

T. Murmu,[a] J. Sienz, S. Adhikari, and C. Arnold
College of Engineering, Swansea University, Singleton Park, Swansea, Wales SA2 8PP, United Kingdom

(Received 12 July 2011; accepted 6 August 2011; published online 25 October 2011)

Buckling behavior of a bonded, uni-axially compressed double-nanoplate-system is investigated in this work. Both the synchronous and asynchronous-type buckling is considered in detail. The two nanoplates are assumed elastically bonded by a polymer resin. The nano-scale effects of nanoplates are dealt with in the analysis by using nonlocal elasticity theory. The theory is utilized for deriving the expressions for a buckling load of a double-nanoplate-system. A simple analytical method is introduced for determining the buckling load of a nonlocal double-nanoplate-system. Explicit closed-form expressions for the buckling load are derived for the case when all four ends are simply supported. Single-layered graphene-sheets are considered for the study. The study highlights that the nonlocal effects considerably influence the buckling behavior of the double-graphene-sheet-system. Unlike the buckling behavior of a single graphene sheet, the double-graphene-sheet-system undergoes both synchronous as well as asynchronous buckling. The nonlocal effects in the double-graphene-sheet-system are higher with increasing values of the nonlocal parameter for the case of synchronous buckling modes than in the asynchronous buckling modes. The increase of the stiffness of the coupling springs in the double-graphene-sheet-system reduces the nonlocal effects during the asynchronous modes of buckling. Different aspect ratios of the double-graphene-sheet-system and higher buckling modes are also considered in the work. © *2011 American Institute of Physics*. [doi:10.1063/1.3644908]

I. INTRODUCTION

One important technological upgradation to the concept of the single nanobeams and nanoplates is that of the complex-nanobeam-systems and complex-nanoplate-systems. Examples of nanobeams include carbon nanotubes[1] and zinc oxide nanotubes;[2] while nanoplates include gold nanoplates,[3] graphene sheets,[4,5] etc. These structures are of nano-dimension scale and possess advanced properties over traditional engineering materials. One simple example of a complex-nanobeam-system is the double-nanobeam-system.[6] The double-nanobeam-systems are utilized in nanooptomechanical systems (NOMS)[7–10] application and in nanocomposites.

Similarly to the complex-nanobeam-system, complex-nanoplate-systems may find applications in nanooptomechanical systems (NOMS) and as an acoustic and vibration isolator. One such example of a complex-nanoplate-system would be the double-nanoplate-system.[11] It should be noted that the present complex systems are different from double-layered system, such as double-walled carbon nanotubes[12] or double-walled graphene systems.[13] These double-walled nanoentities are generally bonded by a constant van der Waal force, which is unlike the double-nanobeam-system or double-nanoplate-system. The double-nanoplate-system would have a different bonding agent of a varying stiffness modulus.

The double-nanoplate systems are important and can be found in nanocomposites structures, such as multiple graphene sheets dispersed in polymer. Though complex-nanoplate-systems, such as double-graphene-sheet-systems, are important in nanodevices and nanocomposites, no works appear related to the elaborate study of its mechanical characteristics. Recently, Murmu and Adhikari[14] and Simsek[15] have addressed the mechanical studies of the double-nanobeam-system.

Understanding the buckling behavior and vibration characteristics of the double-nanoplate-system is important. Recently, the vibration behavior of such systems was considered.[11] In this paper, we discuss the buckling behavioral aspect of the double-nanoplate-systems, considering nonlocal effects.[16–49] The nonlocal elasticity theory is considered. In the nonlocal elasticity theory, the small-scale effects are captured by assuming that the stress at a point is a function of the strains at all points in the domain. The nonlocal theory considers long-range inter-atomic interaction and yields results dependent on the size of a body. In the present problem, two single-layer graphene sheets are considered. The present study can be used beyond graphene sheets as nanoplates. The two single-layered graphene sheets are elastically connected by an enclosing elastic medium, such as polymer resin. Expressions for the buckling load of the system are derived using the nonlocal elasticity theory. An analytical method is introduced for determining the buckling load of the nonlocal double-graphene-sheet-system. Explicit closed-form expressions for buckling load are derived for the case when all four ends are simply supported. Further, this paper presents a unique yet simple method of obtaining the exact solution for the buckling load of the double-graphene-sheet-system. Attention is put on the nonlocal scale effects in synchronous and asynchronous modes of buckling for various coupling springs, aspect ratio, and higher buckling loads. The present study could be useful for nanocomposites.

II. EQUATIONS FOR NONLOCAL ELASTICITY THEORY

In the nonlocal elasticity theory,[16–49] the basic equations for an isotropic linear homogenous nonlocal elastic body, neglecting the body force, are given as

[a]Electronic mail: murmutony@gmail.com. FAX: +44 1792 295676.

$$\sigma_{ij,j} = 0,$$
$$\sigma_{ij}(\mathbf{x}) = \int_{\mathbf{v}} \phi(|\mathbf{x}-\mathbf{x}'|,\alpha) t_{ij} d\mathbf{V}(\mathbf{x}'), \quad \forall \mathbf{x} \in \mathbf{V},$$
$$t_{ij} = H_{ijkl}\varepsilon_{kl},$$
$$\varepsilon_{ij} = \frac{1}{2}(u_{i,j} + u_{j,i}). \tag{1}$$

The terms σ_{ij}, t_{ij}, ε_{kl}, H_{ijkl} are the nonlocal stress, classical stress, classical strain, and fourth order elasticity tensors, respectively. The volume integral is over the region **V** occupied by the body. The kernel function $\phi(|\mathbf{x}-\mathbf{x}'|,\alpha)$ is known as the nonlocal modulus. The nonlocal modulus acts as an attenuation function, incorporating into constitutive equations the nonlocal effects at the reference point **x** produced by local strain at the source $\mathbf{x}'$. The term $|\mathbf{x}-\mathbf{x}'|$ represents the distance in the Euclidean form, and α is a material constant that depends on the internal (e.g., lattice parameter, granular size, distance between the C−C bonds) and external characteristics lengths (e.g., crack length, wave length). Material constant α is defined as $\alpha = e_0 a/\ell$. Here, e_0 is a constant for calibrating the model with experimental results and other validated models. The parameter e_0 is estimated such that the relations of the nonlocal elasticity model could provide satisfactory approximation to the atomic dispersion curves of the plane waves with those obtained from the atomistic lattice dynamics. The terms a and ℓ are the internal (e.g., lattice parameter, granular size, distance between C−C bonds) and external characteristics lengths (e.g., crack length, wave length) of the nanostructure.

Equation (1) is in partial-integral form and generally difficult to solve analytically. Thus, a differential form of the nonlocal elasticity equation is often used. The nonlocal constitutive stress-strain relation can be simplified as[33]

$$(1 - \alpha^2 \ell^2 \nabla^2)\sigma_{ij} = t_{ij}, \tag{2}$$

where ∇^2 is the Laplacian.

Sec. III presents the equation of the double-nanoplate-system under uni-axial compression using this theory of nonlocal elasticity.

III. UNI-AXIALLY COMPRESSED DOUBLE-NANOPLATE-SYSTEM

Consider a nonlocal double-nanoplate-system (NDNPS)[11] bonded by an elastic medium, as shown in Fig. 1. The two nanoplates are assumed to be coupled by polymer resin. The nanoplates are subjected to uni-axial compression. The two nanoplates of the NDNPS are referred to as nanoplate-1 and nanoplate-2.

For mathematical modeling of NDNPS, the elastic medium is represented by vertically distributed identical springs, as shown in Fig. 2. In general, the springs may be used to substitute the elastic medium, forces due to nanooptomechanical effect,[7–10] or Van der Waals forces between the two nanoplates. The springs are assumed to have a stiffness k. Different values of k for different stiffnesses of the polymer matrix can be used for the study. The nanoplates are considered to be of length L and width W. Generally, the two nanoplates are different, where the length, width, mass per unit

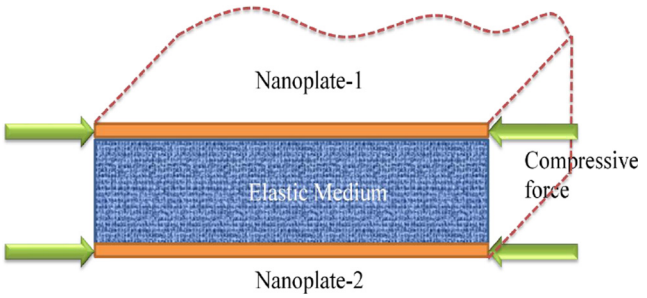

FIG. 1. (Color online) Schematic configuration of uni-axially bonded double-nanoplate-system.

length, and bending rigidity of the ith plate are L_i, W_i, m_i, and D_i $(i = 1, 2)$, respectively. These parameters are assumed to be constant along each nanoplate. The nanoplate-1 and nanoplate-2 are uni-axially compressed by force N_1 and N_2, respectively. The bending displacements over the two nanoplates are denoted by $w_1(x,y,t)$ and $w_2(x,y,t)$, respectively. For generality we have considered w as a function of time also.

The individual governing equations of uni-axially compressed nanoplates for NDNPS, based on the theory of nonlocal elasticity, can be written as

(Nanoplate-1)

$$\begin{aligned} &D_1\nabla^4 w_1(x,y,t) + k[w_1(x,y,t) - w_2(x,y,t)] \\ &\quad - k(e_0a)^2\nabla^2[w_1(x,y,t) - w_2(x,y,t)] \\ &\quad - N_1 w_1''(x,y,t) + N_1(e_0a)^2\nabla^2 w_1''(x,y,t) = 0, \end{aligned} \tag{3}$$

where the bending rigidity of nanoplate-1 is expressed as

$$D_1 = E_1 h_1^3/12(1-\vartheta_1^2). \tag{4}$$

(Nanoplate-2)

$$\begin{aligned} &D_2\nabla^4 w_2(x,y,t) - k[w_1(x,y,t) - w_2(x,y,t)] \\ &\quad + k(e_0a)^2\nabla^2[w_1(x,y,t) - w_2(x,y,t)] \\ &\quad - N_2 w_2''(x,y,t) + N_2(e_0a)^2\nabla^2 w_2''(x,y,t) = 0, \end{aligned} \tag{5}$$

where the bending rigidity of nanoplate-2 is expressed as

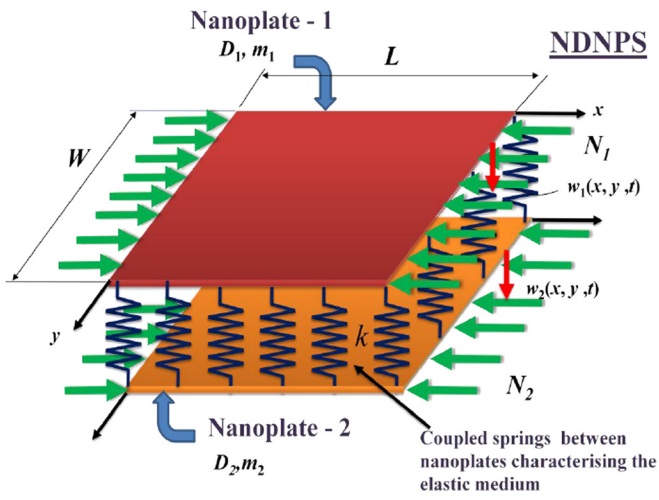

FIG. 2. (Color online) Double-nanoplate-system characterized by coupling vertical springs of stiffness, k.

$$D_2 = E_2 h_2^3/12(1-\vartheta_2^2). \tag{6}$$

The superscript $''$ is double derivative with respect to x.

For the present analysis, we assume that

$$\begin{aligned} &D_1 = D_2 = D \equiv \text{constant}, \\ &N_1 = N_2 = N \equiv \text{constant (uniformly compressed)}. \end{aligned} \tag{7}$$

Substituting the assumptions (Eq. (7)) in Eqs. (3) and (5), we get

(Nanoplate-1)

$$\begin{aligned} &D\nabla^4 w_1(x,y,t) + k[w_1(x,y,t) - w_2(x,y,t)] \\ &\quad - k(e_0a)^2\nabla^2[w_1(x,y,t) - w_2(x,y,t)] \\ &\quad - Nw_1''(x,y,t) + N(e_0a)^2\nabla^2 w_1''(x,y,t) = 0, \end{aligned} \tag{8}$$

(Nanoplate-2)

$$\begin{aligned} &D\nabla^4 w_2(x,y,t) - k(e_0a)^2[w_1(x,y,t) - w_2(x,y,t)] \\ &\quad + k(e_0a)^2\nabla^2[w_1(x,y,t) - w_2(x,y,t)] \\ &\quad - Nw_2''(x,y,t) + N(e_0a)^2\nabla^2 w_2''(x,y,t) = 0. \end{aligned} \tag{9}$$

Next, for the NDNPS, we employ a change of variables by considering $w(x,y,t)$ as the relative displacement of the nanoplate-1 with respect to the nanoplate-2,[11]

$$w(x,y,t) = w_1(x,y,t) - w_2(x,y,t), \tag{10}$$

such that, for nanoplate-1, the displacement is expressed as

$$w_1(x,y,t) = w(x,y,t) + w_2(x,y,t). \tag{11}$$

Subtracting Eq. (8) from (9) would lead to

$$\begin{aligned} &D\nabla^4[w_1(x,y,t) - w_2(x,y,t)] + 2k[w_1(x,y,t) - w_2(x,y,t)] \\ &\quad - 2k(e_0a)^2\nabla^2[w_1(x,y,t) - w_2(x,y,t)] \\ &\quad - N[w_1''(x,y,t) - w_2''(x,y,t)] + N(e_0a)^2\nabla^2 \\ &\quad \times [w_1''(x,y,t) - w_2''(x,y,t)] = 0. \end{aligned} \tag{12}$$

Using Eq. (10) in Eq. (12) and Eq. (9),

$$\begin{aligned} &D\nabla^4 w(x,y,t) + 2kw(x,y,t) - 2k(e_0a)^2\nabla^2 w(x,y,t) \\ &\quad - Nw''(x,y,t) + N(e_0a)^2\nabla^2 w''(x,y,t) = 0, \end{aligned} \tag{13}$$

$$\begin{aligned} &D\nabla^4 w_2(x,y,t) - Nw_2''(x,y,t) + N(e_0a)^2\nabla^2 w_2''(x,y,t) \\ &\quad = k(e_0a)^2 w(x,y,t) - k(e_0a)^2\nabla^2 w(x,y,t). \end{aligned} \tag{14}$$

For the present analysis of coupled NDNPS, we see the simplicity in using Eqs. (13) and (14). It should be noted that, when the nonlocal effects are ignored ($e_0a = 0$) and a single nanoplate is considered, the above equations revert to the equations of classical Kirchhoff's plate theory.

Now, we present the mathematical expressions of the boundary conditions of the NDNPS. It is assumed that all the edges in the nanoplate system are simply supported. The use of boundary conditions is described here. At each end of the nanoplates in NDNPS, the displacement and the nonlocal moments are considered to be zero. They can be mathematically expressed as[11]

(Nanoplate-1)

Displacement condition

$$\begin{aligned} &w_1(0,y,t) = 0; \quad w_1(L,y,t) = 0; \quad w_1(x,0,t) = 0; \\ &w_1(x,W,t) = 0, \end{aligned} \tag{15}$$

Nonlocal moment condition

$$\begin{aligned} &M_1(0,y,t) = 0; \quad M_1(L,y,t) = 0; \quad M_1(x,0,t) = 0; \\ &M_1(x,W,t) = 0. \end{aligned} \tag{16}$$

(Nanoplate-2)

Displacement condition

$$\begin{aligned} &w_2(0,y,t) = 0; \quad w_2(L,y,t) = 0; \quad w_2(x,0,t) = 0; \\ &w_2(x,W,t) = 0, \end{aligned} \tag{17}$$

Nonlocal moment condition

$$\begin{aligned} &M_2(0,y,t) = 0; \quad M_2(L,y,t) = 0; \quad M_2(x,0,t) = 0; \\ &M_2(x,W,t) = 0. \end{aligned} \tag{18}$$

Now, we use Eq. (10) in the displacement boundary conditions in Eqs. (15) and (17),

$$w(0,y,t) = w_1(0,y,t) - w_2(0,y,t) = 0, \tag{19a}$$

$$w(L,y,t) = w_1(L,y,t) - w_2(L,y,t) = 0, \tag{19b}$$

$$w(x,0,t) = w_1(x,0,t) - w_2(x,0,t) = 0, \tag{19c}$$

$$w(x,W,t) = w_1(x,W,t) - w_2(x,W,t) = 0. \tag{19d}$$

Similarly, using Eq. (10) in the nonlocal moment boundary conditions in Eqs. (16) and (18),

$$M(0,y,t) = M_1(0,y,t) - M_2(0,y,t) = 0, \tag{20a}$$

$$M(a,y,t) = M_1(L,y,t) - M_2(L,y,t) = 0, \tag{20b}$$

$$M(x,0,t) = M_1(x,0,t) - M_2(x,0,t) = 0, \tag{20c}$$

$$M(x,b,t) = M_1(x,W,t) - M_2(x,W,t) = 0. \tag{20d}$$

IV. BUCKLING STATES OF DOUBLE-NANOPLATE-SYSTEM

Here, we explicitly consider the different cases of nonlocal buckling, which would happen on the double-nanoplate-system[11] under uni-axial compressive force. The cases studied will be nanoplates buckling with out-of-phase (asynchronous) sequence, in-phase (synchronous) sequence, and when one of the nanoplates is considered to be fixed.

A. Both nanoplates buckling asynchronously; ($w_1 - w_2 \neq 0$)

Figure 3 shows the configuration of the double-nanoplate-system with the asynchronous (out-of-phase) sequence of buckling ($w_1 - w_2 \neq 0$). It should be noted that the figure represents the first out-of-phase buckling phenomenon. In an

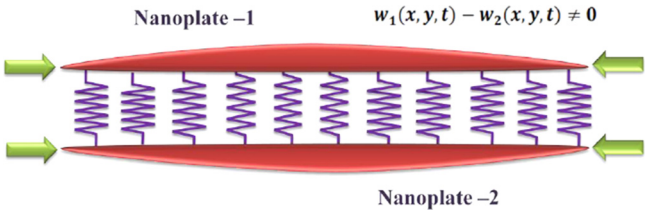

FIG. 3. (Color online) Asynchronous type buckling of the double-nanoplate-system.

out-of-phase sequence of buckling, the nanoplates are buckled in opposite directions.

In this section, we evaluate the buckling load for the out-of-phase (asynchronous) type buckling. We will use Eq. (13) for the buckling solution of the double-nanoplate-system. The system can be considered as independent of time.

We assume the buckling mode of the double-nanoplate-system as[50]

$$w = W_{mn} sin\frac{m\pi x}{L} sin\frac{n\pi y}{W}. \tag{21}$$

Substituting Eq. (21) into Eq. (13) yields

$$D\left[\left(\frac{m\pi}{L}\right)^2+\left(\frac{n\pi}{W}\right)^2\right]^2 w + 2kw + 2k(e_0a)^2\left[\left(\frac{m\pi}{L}\right)^2+\left(\frac{n\pi}{W}\right)^2\right]w + N\left(\frac{m\pi}{L}\right)^2 w + N(e_0a)^2\left(\frac{m\pi}{L}\right)^2\left[\left(\frac{m\pi}{L}\right)^2+\left(\frac{n\pi}{W}\right)^2\right]w = 0. \tag{22}$$

For the sake of simplicity, we introduce the following parameters:

$$K = \frac{kL^4}{D}; \quad \widehat{N} = -\frac{NL^2}{D}; \quad \mu = \frac{e_0a}{L}; \quad R = \frac{L}{W}. \tag{23}$$

Using Eqs. (23) and (22) we get the expression of buckling load in an out-of-phase sequence of the nonlocal double nanoplate system as

$$\widehat{N} = \frac{[(m\pi)^2 + R^2(n\pi)^2]^2 + 2K + 2K\mu^2[(m\pi)^2 + R^2(n\pi)^2]}{(m\pi)^2[1 + \mu^2[(m\pi)^2 + R^2(n\pi)^2]]}. \tag{24}$$

B. Both nanoplates buckling synchronously; ($w_1 - w_2 = 0$)

Here, we will consider the in-phase (synchronous) sequence of buckling of the double-nanoplate-system under uni-axial compression. The schematic illustration is shown in Fig. 4, which is the first synchronous type buckling. For the present nanoplate system, the relative displacements between the two nanoplates are absent, i.e., $\boldsymbol{w_1 - w_2 = 0}$. The nanoplates are buckled in the same direction (synchronous). In the synchronous buckling state, the double nanoplate system can be considered to be as one of the nanoplates (viz. nanobeam-2).

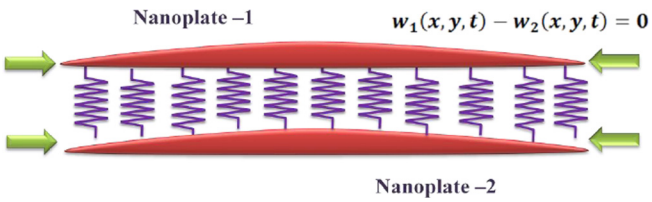

FIG. 4. (Color online) In-phase type buckling behavior of the double-nanoplate-system.

Here, we solve Eq. (14) for the synchronous sequence of buckling. We apply the same procedure as earlier for solving Eq. (13). The buckling load of the nonlocal double-nanoplate-system is evaluated as

$$\widehat{N} = \frac{[(m\pi)^2 + R^2(n\pi)^2]^2}{(m\pi)^2\left[1 + \mu^2[(m\pi)^2 + R^2(n\pi)^2]\right]}. \tag{25}$$

Here, we see for this case that the buckling phenomenon in the double-nanoplate-system is independent of the stiffness of the connecting springs and, therefore, the double-nanoplate-system can be effectively treated as a single nanoplate.

C. One nanoplate is fixed in the double-nanoplate-system ($w_2 = 0$)

Consider the case of the double-nanoplate-system when one of the two nanoplates (viz. nanoplate-2) is stationary ($w_2 = 0$). The schematic configuration of the NDNPS is shown in Fig. 5.

We utilize the equations from the nonlocal elasticity, and the governing equation for the NDNBS in this case reduces to

$$D\nabla^4 w(x,y,t) + kw(x,y,t) - k(e_0a)^2\nabla^2 w(x,y,t) - Nw''(x,y,t) + N(e_0a)^2\nabla^2 w''(x,y,t) = 0. \tag{26}$$

Here, it is worth noting that, in this case, the double-nanoplate-system behaves as if the nanoplate is embedded or supported on an elastic medium or other forces in nanoscale (Fig. 5). The elastic medium can be modeled as a Winkler elastic foundation. The stiffness of the elastic medium is denoted by k. By following the same procedure as the solution of Eq. (13), the explicit nonlocal buckling load of the double nanoplate can be easily obtained. The buckling load is evaluated as

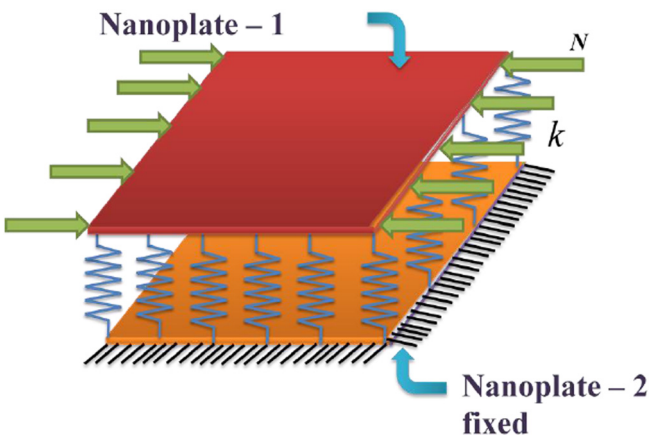

FIG. 5. (Color online) Buckling behavior of uni-axially compressed NDNPS with one nanoplate stationary.

$$\widehat{N} = \frac{[(m\pi)^2 + R^2(n\pi)^2]^2 + K + K\mu^2[(m\pi)^2 + R^2(n\pi)^2]}{(m\pi)^2[1 + \mu^2[(m\pi)^2 + R^2(n\pi)^2]]}. \tag{27}$$

In fact, when one of the nanoplate (viz. nanoplate-2) in NDNPS is fixed ($w_2 = 0$), the double-nanoplate-systems behave as the nanoplate on an elastic medium.

V. RESULTS AND DISCUSSION

A. Coupled double-graphene-sheet-system

As an illustration, the properties of the nanoplates are considered as those of single-walled graphene sheets. The two graphene sheets (GS) are coupled by the embedded polymer matrix (Fig. 6). The bonded double-graphene-sheet-system is uni-axially compressed. The Young's modulus of the GS is considered as $E = 1.06$ TPa; the Poisson ratio is $\vartheta = 0.25$. The thickness of the GS is taken as $h = 0.34$ nm.

The nonlocal double-plate theory for NDNPS illustrated here is a generalized theory and can be applied for the buckling analysis of coupled graphene sheets (multiple-walled), gold nanoplates, etc. The reliability of the nonlocal elasticity theory in the analysis of nanostructures (nanotubes and graphene sheet) can be observed in various earlier works.[16–49]

The buckling results of the NDNPS are presented in terms of the buckling load parameters (Eq. (23)). The nonlocal parameter and the stiffness of the springs are computed, as given in Eq. (23). Different values of the spring parameters, K, are considered. Spring stiffness represents the stiffness of the enclosing elastic medium. Both high and large stiffnesses of springs are assumed. Values of K range from 10 to 100. Both the graphene sheets (GS-1 and GS-2) are assumed to have the same geometrical and material properties. In general, the nonlocal parameters may be taken as $e_0 = 0.39$ (Ref. 16) and $a = 0.142$ nm (distance between carbon-carbon atoms). For carbon nanotubes and graphenes, the range of $e_0 a = 0-2.0$ nm has been widely used. In the present study, we take the scale coefficient μ or nonlocal parameter in the similar range as $\mu = 0-1$.[27]

B. Effect of small-scale on NDNPS undergoing compression

To see the influence of the small-scale on the natural buckling load of the coupled-graphene sheet-systems, curves have been plotted for the buckling load parameter and scale coefficient (nonlocal parameter, μ).

To signify the small-scale effect, we introduce a parameter buckling load reduction percent (BLRP). Buckling load reduction percent (BLRP) is defined as

$$\text{BLRP} = 100 \times \left(\frac{\widehat{N}_{Local} - \widehat{N}_{Nonlocal}}{\widehat{N}_{Local}} \right). \tag{28}$$

Figure 7 shows the variation of the BLRP with the scale coefficient for different cases of NDNPS. The results for the load reduction parameter are in the dimensionless form, as in Eq. (23). The stiffness parameter of the coupling springs between the GS is assumed to be constant ($K = 10$). From the figure (Fig. 7), it can be observed that, as the scale coefficient μ increases, the BLRP increases. This implies that, for increasing scale coefficient, the value of load parameter decreases. The reduction in load parameter is due to the assimilation of small-scale effects in the NDNPS in the material properties of the graphene sheets. The small-scale effect reduces the stiffness of the material and, hence, the comparative lower buckling load. Therefore, by the nonlocal elastic model, the size effects are reflected in the NDNPS.

Three different cases of NDNPS are considered. Case 1, case 2, and case 3 depict the conditions (i) when both the GS buckles in the out-of-phase (asynchronous) sequence ($w_1 - w_2 \neq 0$), (ii) when one of the GS in NDNPS is stationary ($w_2 = 0$), and (iii) when both the GS buckles with in-phase (synchronous) sequence ($w_1 - w_2 = 0$), respectively. Comparing the three cases of the coupled-graphene-sheet-system, we observe that the BLRP for case 3 (in-phase buckling behavior) is larger than the BLRP for case 1 (out-of-phase

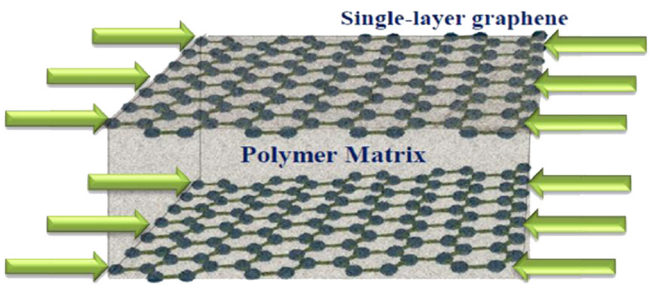

FIG. 6. (Color online) Uni-axially compressed bonded double-graphene-sheet-system.

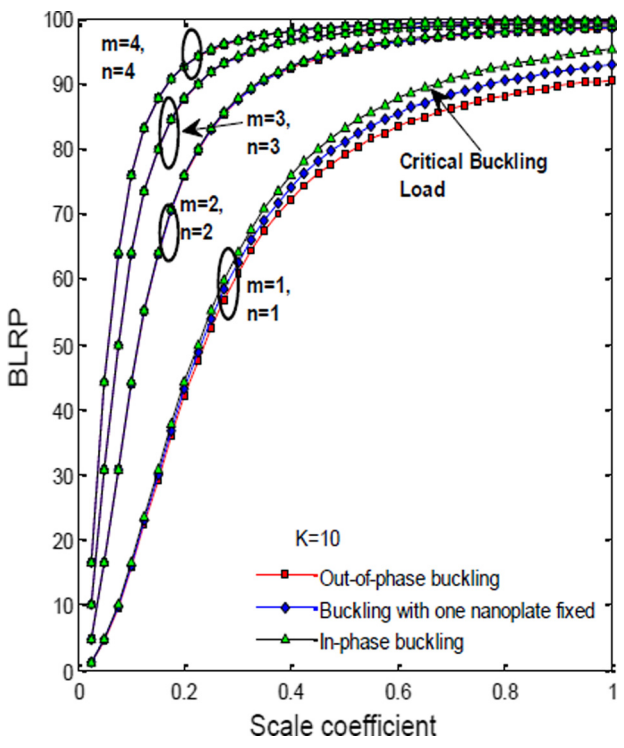

FIG. 7. (Color online) Effect of scale coefficient on buckling load reduction percent (BLRP).

buckling behavior) and case 2 (one-GS fixed). In other words, the scale coefficient significantly reduces the in-phase buckling load (thus, higher BLRP) compared to the other cases considered. The relatively higher BLRP in case 3 is due to the absence of coupling effect of the spring and the two nanoplates (GSs).

In addition, it can be seen that the values of the BLRP for case 2 (one-GS fixed) is larger than the values of the BLRP for case 1 (out-of-phase buckling behavior). For case 2, the coupled-graphene-sheet-system becomes similar to the buckling behavior characteristic of the single GS with the effect of elastic medium. In case 3 (in-phase buckling behavior), the load reduction parameter is relatively less, because the NDNPS becomes independent of the effect of the spring stiffness. For case 3, the NDNPS becomes similar to the buckling response of the single GS without the effect of the elastic medium. In other words, the whole NDNBS can be treated as a buckled single GS, and the coupling internal structure is effectless.

In general, it is worth noticing that the small-scale effects in NDNPS are higher with an increasing nonlocal parameter in the in-phase buckling behavior than in the out-of-phase buckling behavior. This is because the stiffness of the springs in the out-of-phase buckling behavior reduces the nonlocal effects.

Higher modes of buckling in the NDNPS (i.e., $m=1$, $n=1$; $m=2$, $n=2$; $m=3$, $n=3$; and $m=4$, $n=4$) are also depicted in the Fig. 7. It is observed that small-scale effects are higher for higher modes of buckling, $m=1$, $n=1<m=2$, $n=2<m=3$, $n=3<m=4$, $n=4$. Further, it is important to note that, with increasing modes of buckling, the difference among the (i) out-of-phase (asynchronous) sequence ($w_1 - w_2 \neq 0$), (ii) in-phase (synchronous) sequence ($w_1 - w_2 = 0$) of buckling, and (iii) one nanoplate stationary reduces. It should be noted that the modes for case 1 and case 3 can be referred to as submodes of original modes.

C. Effect of stiffness of coupling springs in NDNPS

To illustrate the influence of stiffness of the springs on the buckling load of the coupled-GS-systems, curves have been plotted for the BLRP against the scale coefficient. Spring stiffness represents the stiffness of the enclosing elastic medium (polymer resin). Different values of the stiffness parameter of the coupling springs are considered. Figures 8–10 depict the stiffness of the springs on the BLRP of coupled systems. The stiffness parameter of the coupling springs are taken as $K=0$, 50, and 100, respectively. Aspect ratio (L/W) is taken as unity. From the figure, it is noticed that, as the stiffness parameter of the coupling springs increases, the BLRP decreases.

Considering all values of the stiffness parameter and comparing the three cases of the coupled-GS system, it is noticed that the BLRP for case 3 (in-phase buckling) is larger than the BLRP for case 1 (out-of-phase buckling) and case 3 (one-GS fixed). These different changes of BLRP with the increasing scale coefficient for the three different cases are more amplified as the stiffness parameter of the springs increases. For case 1 (out-of-phase buckling) and case 2 (one-GS-fixed), the BLRP reduces with increasing values of

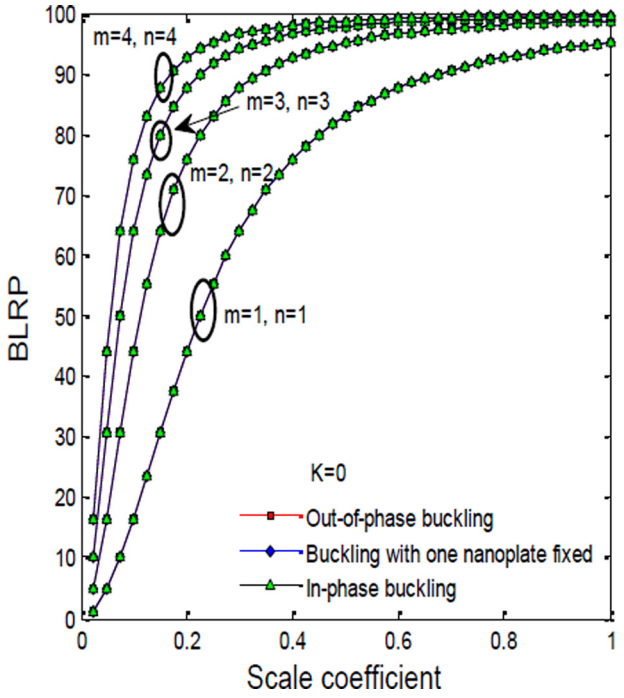

FIG. 8. (Color online) Effect of scale coefficient on BLRP of NDNPS for $K=0$.

stiffness parameter. This observation implies that case 1 (out-of-phase buckling) and case 2 (one GS fixed) are less affected by scale-effects. Comparing case 1 and case 2, it can be seen that the BLRP is less for out-of-phase buckling than for buckling in case 2. Thus, the out-of-phase buckling is less affected by the small-scale or nonlocal effects. This out-of-phase buckling can be attributed to the fact that the coupling springs in the vibrating system dampens the nonlocal effects. The in-phase buckling of the coupled-system is unchangeable with increasing stiffness of springs. This is

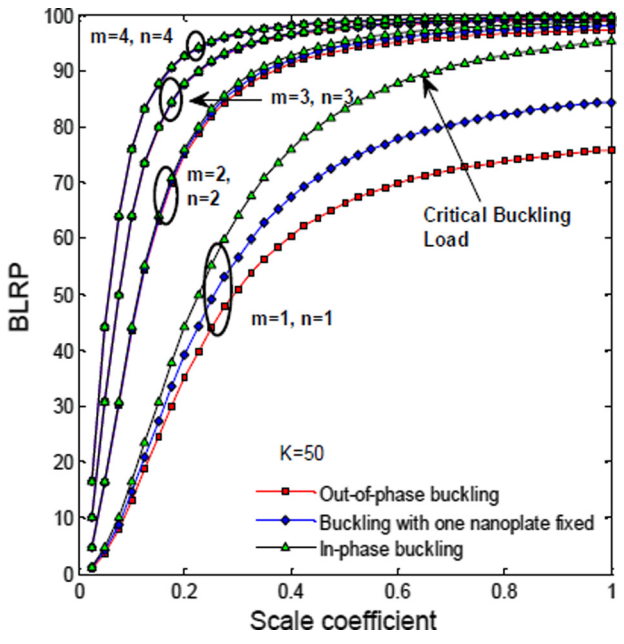

FIG. 9. (Color online) Effect of scale coefficient on BLRP of NDNPS for $K=50$.

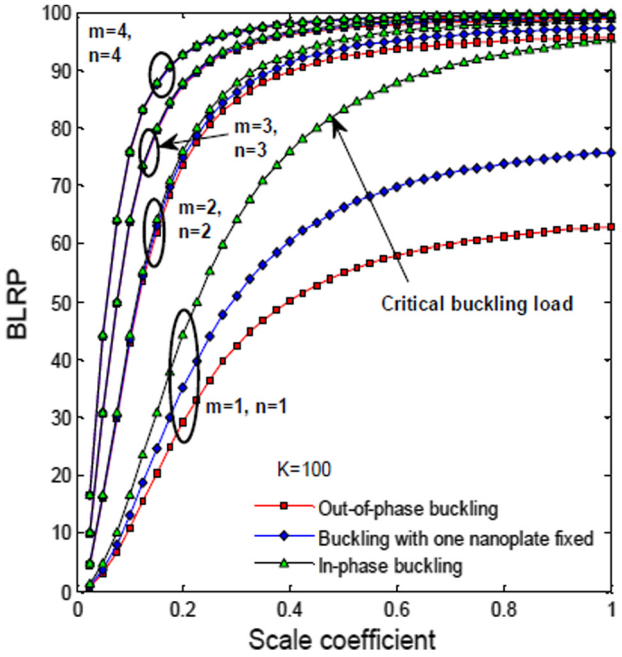

FIG. 10. (Color online) Effect of scale coefficient on BLRP of NDNPS for $K = 100$.

due to the in-phase buckling mode of behavior. For the in-phase type of buckling, the coupled system behaves as a single graphene without the effect of an internal elastic medium. In other words, the whole coupled system can be treated as a single nanoelement, and the coupling internal structure is affected less. In summary, it should be noted that the in-phase buckling of the coupled-system is more affected by small-scale effects compared to out-of-phase buckling.

D. Effect of aspect ratio on NDNPS

Next, we illustrate the influence of aspect ratios (L/W) of the nanoplates (GS) on the buckling load of the coupled-GS-systems. The GSs are assumed to be coupled by a polymer matrix of stiffness $K = 100$. Curves have been plotted for the BLRP against the scale coefficient for different aspect ratios. Different values of aspect ratios of the NDNPS are considered. Figures 11–13 depict the effect of aspect ratio on the BLRP of coupled systems. The aspect ratios are taken as $L/W = 0.2$, 0.4, and 0.8.

From Figs. 11–13, we see that, with the increase of aspect ratios (L/W) of NDNPS, the BLRP for all cases of buckling increases. It is noticed that the difference between the in-phase type buckling, out-of-phase type buckling, and buckling with one GS fixed become less for increasing aspect ratios (L/W) of NDNPS. Thus, it can be concluded that,

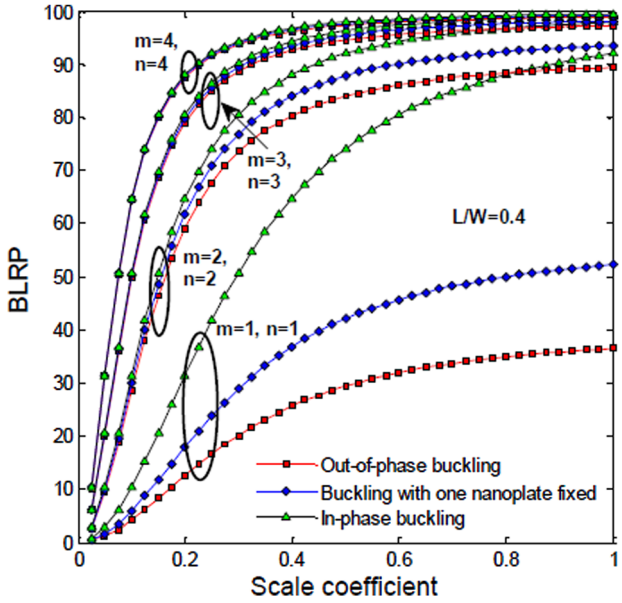

FIG. 12. (Color online) Effect of scale coefficient on BLRP of NDNPS for $L/W = 0.4$.

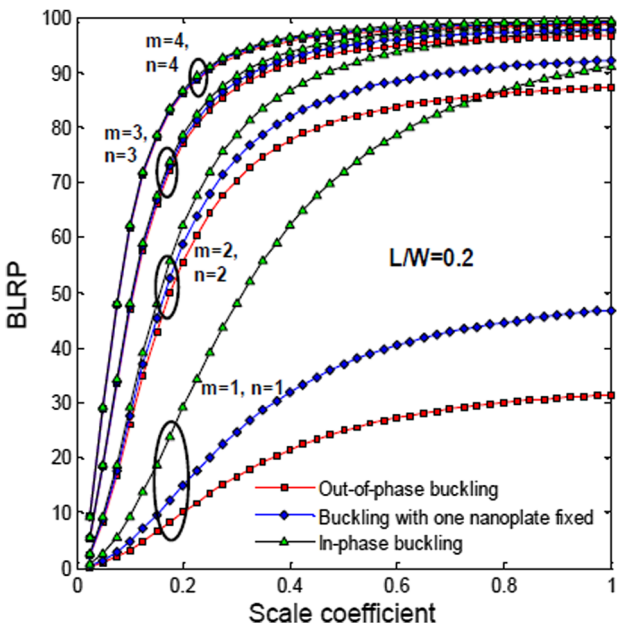

FIG. 11. (Color online) Effect of scale coefficient on BLRP of NDNPS for $L/W = 0.2$.

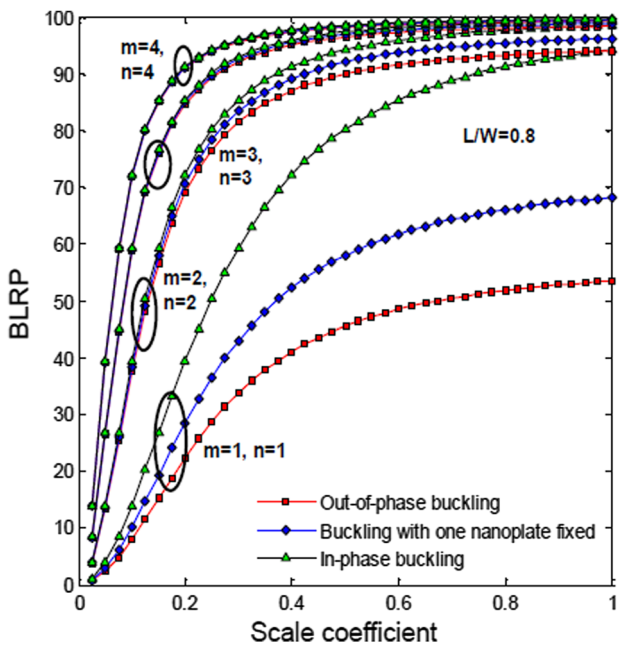

FIG. 13. (Color online) Effect of scale coefficient on BLRP of NDNPS for $L/W = 0.8$.

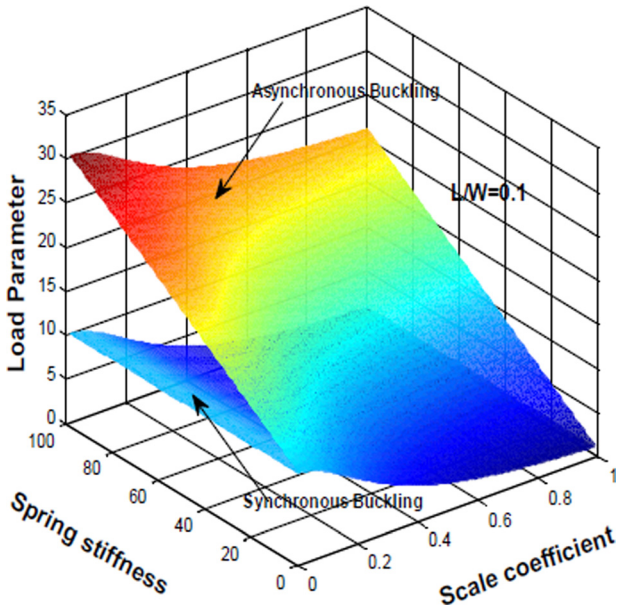

FIG. 14. (Color online) The variation of the buckling load parameter for the asynchronous and synchronous buckling of NDNPS as a function of the spring stiffness (K) and the scale-coefficient (μ) with L/W = 0.1.

although the small scale effects are more in higher aspect ratios (L/W) of NDNPS, the effect of the stiffness of coupling springs are reduced in higher aspect ratios of NDNPS, and thus, the difference in curves between the in-phase type buckling, out-of-phase type buckling, and buckling with one GS fixed become less for higher aspect ratios of NDNPS.

Finally, for the comprehension of the buckling phenomenon of NDNPS with small-scale effects, the buckling load parameter of the double nanoplate system for different nonlocal parameters (scale coefficient) and spring stiffness parameters (K) are plotted in a three-dimensional graph. Three different aspect ratios of the NDNPS are considered. The stiffness parameter K of the coupling springs are considered in the range of 0−100. Figures 14–16 show the plots for the aspect ratio of L/W = 0.1, 0.5, and 1.0, respectively. The nonlocal parameter or scale coefficient μ is varied from

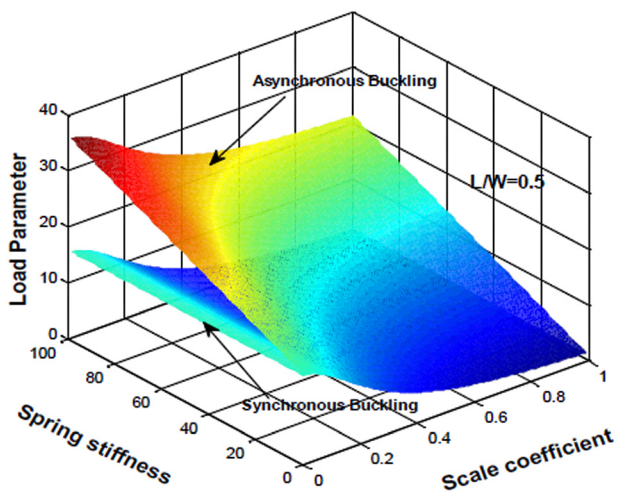

FIG. 15. (Color online) The variation of the buckling load parameter for the asynchronous and synchronous buckling of NDNPS as a function of the spring stiffness (K) and the scale-coefficient (μ) with L/W = 0.5.

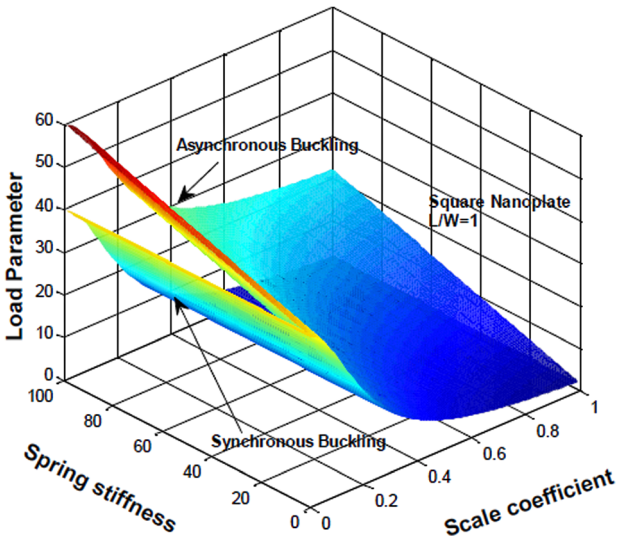

FIG. 16. (Color online) The variation of the buckling load parameter for the asynchronous and synchronous buckling of NDNPS as a function of the spring stiffness (K) and the scale-coefficient (μ) with L/W = 1.0 (square plate).

0 to 1. From Fig. 14, it is observed that the increase of the scale coefficient has a reducing effect on the nonlocal buckling load of the NDNPS. The stiffness of the springs has a reducing effect on the small-scale effects of the NDNPS. It should be noted that, for in-phase buckling, the loads are independent of the coupling springs. Also, it is concluded from the figure that the difference between the asynchronous and synchronous buckling decreases with increasing aspect ratios (Figs. 15 and 16).

VI. CONCLUSIONS

In this article, expressions for buckling of the double-nanoplate-system are established within the framework of Eringen's nonlocal elasticity. An analytical method is introduced for determining the buckling load of the nonlocal double-nanoplates-system (NDNPS). Explicit closed-form expressions for buckling load are derived for the case when all four ends are simply supported. Two single-layered graphene sheets coupled by a polymer matrix are considered for the study. The study highlights that the small-scale effects considerably influence the buckling load of NDNPS. The small-scale effects in NDNPS are higher with increasing values of the nonlocal parameter for the case of synchronous modes of buckling than in the asynchronous modes of buckling. The increase of the stiffness of the coupling springs in NDNPS reduces the small-scale effects during the asynchronous modes of buckling. This work may provide an analytical scale-based nonlocal approach, which could serve as the starting point for further investigation of more complex n-nanoplates systems undergoing instability.

[1]S. Iijima, Nature **354**, 56 (1991).
[2]R. M. Wang, Y. J. Xing, J. Xu, and D. P. Yu, New J. Phys. **5**, 115 (2003).
[3]Y. Shao, Y. Jin, and S. Dong, Chem. Commun. (Cambridge) **9**, 1104 (2004).
[4]A. K. Geim and K. S. Novoselov, Nature Mater. **6**, 183 (2007).
[5]A. K. Geim, Science **324**, 1530 (2009).

[6]T. Murmu and S. Adhikari, J. Appl. Phys. **108**, 083514 (2010).
[7]I. W. Frank, P. B. Deotare, M. W. McCutcheon, and M. Loncar, Opt. Express **18**, 8705 (2010).
[8]M. Eichenfield, R. Camacho, J. Chan, K. J. Vahala, and O. Painter, Nature **459**, 550 (2009).
[9]P. B. Deotare, M. W. McCutcheon, I. W. Frank, M. Khan, and M. Loncar, Appl. Phys. Lett. **95**, 031102 (2009).
[10]Q. Lin, J. Rosenberg, D. Chang, R. Camacho, M. Eichenfield, K. J. Vahala, and O. Painter, Nat. Photonics **4**, 236 (2010).
[11]T. Murmu and S. Adhikari, Composites, Part B **42**, 1901 (2011).
[12]T. P. Chang and M. F. Liu, Physica E **43**, 1419 (2011).
[13]Y. Chandra, R. Chowdhury, F. Scarpa, and S. Adhikari, Thin Solid Films **519**, 6026 (2011).
[14]T. Murmu and S. Adhikari, Phys. Lett. A **375**, 601 (2011).
[15]M. Simsek, Comput. Mater. Sci. **778**, 2112 (2011).
[16]A. C. Eringen, J. Appl. Phys. **54**, 4703 (1983).
[17]P. Lu, H. P. Lee, C. Lu, and P. Q. Zhang, J. Appl. Phys. **99**, 073510 (2006).
[18]J. Yang, L. L. Ke, and S. Kitipornchai, Physica E **42**, 1727 (2010).
[19]T. Murmu and S. C. Pradhan, Physica E **41**, 1232 (2009).
[20]T. Murmu and S. C. Pradhan, Comput. Mater. Sci. **46**, 854 (2009).
[21]T. Murmu and S. C. Pradhan, Comput. Mater. Sci. **47**, 721 (2010).
[22]C. M. Wang and W. H. Duan, J. Appl. Phys. **104**, 014303 (2008).
[23]J. N. Reddy and S. D. Pang, J. Appl. Phys. **103**, 023511 (2008).
[24]J. Peddieson, G. G. Buchanan, and R. P. McNitt, Int. J. Eng. Sci. **41**, 305 (2003).
[25]C. M. Wang, Y. Y. Zhang, S. S. Ramesh, and S. Kitipornchai, J. Phys. D **39**, 3904 (2006).
[26]P. Lu, J. Appl. Phys. **101**, 073504 (2007).
[27]M. Aydogdu, Physica E **41**, 861 (2009).
[28]H. Heireche, A. Tounsi, A. Benzair, M. Maachou, and E. A. Adda Bedia, Physica E **40**, 2791 (2008).
[29]M. Aydogdu, Physica E **41**, 1651 (2009).
[30]L. Wang, Physica E **41**, 1835 (2009).
[31]Y. Yan, W. Q. Wang, and L. X. Zhang, Appl. Math. Model. **34**, 3422 (2010).
[32]F. Khademolhosseini, R. K. N. D. Rajapakse, and A. Nojeh, Comput. Mater. Sci. **48**, 736 (2010).
[33]J. N. Reddy, Int. J. Eng. Sci. **45**, 288 (2007).
[34]C. M. Wang, S. Kitipornchai, C. W. Lim, and M. Eisenberger, J. Eng. Mech. **134**, 475 (2008).
[35]J. C. Niu, C. W. Lim, and A. Y. T. Leung, Proc. Inst. Mech. Eng., Part C: J. Mech. Eng. Sci. **223**, 2451 (2009).
[36]M. Simsek, Physica E **43**, 182 (2010).
[37]M. Simsek, Steel Compos. Struct. **11**, 59 (2011).
[38]H. Heireche, A. Tounsi, and A. Benzair, Nanotechnology **19**, 185703 (2008).
[39]H. Heireche, A. Tounsi, A. Benzair, and I. Mechab, J. Appl. Phys. **104**, 014301 (2008).
[40]A. Tounsi, H. Heireche, and E. A. Adda Bedia, J. Appl. Phys. **105**, 126105 (2009).
[41]A. Tounsi, H. Heireche, A. Benzair, and I. Mechab, J. Phys.: Condens. Matter **21**, 448001 (2009).
[42]C. W. Lim and C. M. Wang, J. Appl. Phys. **101**, 054312 (2007).
[43]S. C. Pradhan and T. Murmu, J. Appl. Phys. **105**, 124306 (2009).
[44]M. Aydogdu and S. Filiz, Physica E **43**, 1229 (2011).
[45]S. Filiz and M. Aydogdu, Comput. Mater. Sci. **49**, 619 (2010).
[46]T. Aksencer and M. Aydogdu, Physica E **43**, 954 (2011).
[47]Y. Z. Wang, F. M. Li, and K. Kishimoto, Physica E **42**, 1356 (2010).
[48]S. Narendar and S. Gopalakrishnan, Physica E **43**, 1185 (2011).
[49]S. Narendar, R Mahapatra, and S. Gopalakrishnan, Int. J. Eng. Sci. **49**, 509522 (2011).
[50]R. M. Jones, Buckling of Bar, Plates and Shells (Bull Ridge Corporation, Blacksburg, VA, 2006).